

Study of Interaction of High Power Plasma Stream with Lithium–Carbon Composites¹

A.A. Shoshin^{***}, A.V. Burdakov^{****}, B.F. Bayanov^{*}, I.A. Ivanov^{***}, K.N. Kuklin^{*}, P.A. Simonov^{****}, V.N. Snytnikov^{****}, S.V. Polosatkin^{***}, and V.V. Postupaev^{***}

^{*}*Budker Institute of Nuclear Physics SB RAS, 11, Lavrent'eva ave., Novosibirsk, 630090, Russia*
 Phone: +7(383)329-40-65, Fax: +7(383) 330-71-63, E-mail: shoshin@inp.nsk.su

^{**}*Novosibirsk State University, 2, Pirogova str., Novosibirsk, 630090, Russia*

^{***}*Novosibirsk State Technical University, 20, Marksa ave., Novosibirsk, 630092, Russia*

^{****}*Boreskov Institute of Catalysis SB RAS, 5, Lavrent'eva ave., Novosibirsk, 630090, Russia*

Abstract – First results on the use of lithium-covered structures with carbon-based substrates in the multimirror trap GOL-3 are presented. Main aim of this program is search for an optimal material of plasma-facing components which should withstand transient high power loads during the device operation. Stability of lithium layer heated by the plasma stream above the melting point was studied for different substrate materials, including graphites and sibunit-based composite. Special material test station equipped with a set of optical diagnostics of lithium plasma was developed. Design of first trial targets and parameters of surface plasma at $\sim 2 \text{ MJ/m}^2$ energy density are discussed.

1. Introduction

Development of large-scale fusion devices meets a challenge of a proper choice of a plasma-facing material which can durably withstand high particle and power loads from fusion plasma. This problem is well understood (see, e.g., [1]) and fusion community spent many efforts for simulation experiments [2]. Requirements for the candidate material of high-power-loaded plasma-facing components are contradictory. Such material must withstand repetitive loads from transient plasma events like ELMs, it should have low sputtering rate, low atomic number, high melting point and no chemical compounds with hydrogen. Up to date, no universal solution found.

Recently considerable progress was achieved with composite structures based on lithium-filled tungsten capillary-porous materials. Plasma-facing surface of such structure is covered by a thin liquid lithium layer which self-repairs during the operation due to surface tension and capillary feed through the porous structure [3–5]. Improvement of plasma parameters with the introduction of lithium limiter was initially demonstrated in T-11 [6] and then in several other tokamaks.

Problems of plasma contamination by carbon and high-Z impurities, accumulation of carbon dust and redeposited carbon are important for operation of the

multimirror trap GOL-3 which has several in-chamber graphite elements. Energy density at a surface of a solid in GOL-3 experiments can reach $\sim 10 \text{ MJ/m}^2$ with an exposure time $< 1 \text{ ms}$. These parameters are close to design specifications for ITER divertor load. However, volumetric energy deposition of fast electrons of the relativistic beam in GOL-3 makes use of mentioned capillary structures difficult due to high stopping power of tungsten and its consequent overheating. Thus, the decision was made to start development of technology of carbon-based lithium-filled composite structures for GOL-3.

First results of tests of carbon-lithium samples are presented in the paper. Lithium-covered graphite and lithium-filled sibunit[®] [7] and graphite targets were exposed to plasma stream of reduced down to $\sim 2 \text{ MJ/m}^2$ energy density. Even at reduced energy load the surface layer of lithium gets heated above the melting, so the considerable density of lithium plasma was expected. At this stage, most attention was concentrated on a technology of such materials and on development of a start set of optical diagnostics of lithium plasma near the surface.

2. Experimental conditions

Primary task of the GOL-3 facility in Budker Institute of Nuclear Physics is development of a multiple mirror magnetic confinement scheme for fusion. This approach differs from other magnetic confinement schemes by higher plasma density and multimirror (corrugated) magnetic field of linear topology. Principal feature of GOL-3 experiments is the use of a high-power relativistic electron beam for fast collective plasma heating. In the discussed experiments the beam parameters were 0.8 MeV, $\sim 30 \text{ kA}$, $12 \mu\text{s}$, $\sim 120 \text{ kJ}$. The temperature of deuterium plasma of $\sim 10^{21} \text{ m}^{-3}$ density was 2–3 keV [8].

The relativistic electrons beam loses $\sim 40\%$ of initial kinetic energy in average during the collective relaxation in the plasma. Several linked collective processes occur during the beam relaxation which

¹ The work was partially supported by SB RAS (Project No. 112), RFBR (No. 08-02-13570), Russian Science Support Foundation (Nos. CRDF Y4-P-08-09, RNP.2.2.2.3.1003, and MK-4229.2007.2).

results in fast effective heating of plasma electrons and ions. The energy confinement time reaches ~ 1 ms in best regimes. The relaxed beam electrons and plasma exhaust from the trap are dumped to the exit beam receiver which is placed in a decreasing magnetic field in order to reduce energy load to the collector below the safe margin.

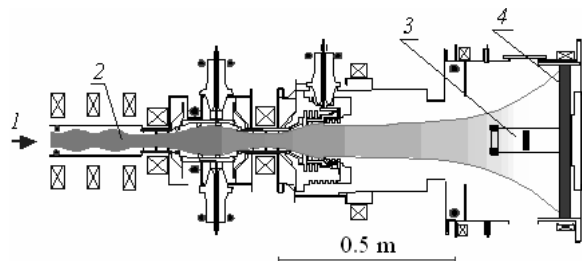


Fig. 1. Layout of experiments on Li-carbon targets exposing by hot-plasma stream on GOL-3 facility: 1 – exhaust of plasma; 2 – end of multi-mirror trap; 3 – target; 4 – plasma dump

Energy density in the exhaust plasma stream reaches ~ 30 MJ/m² in the exit mirror and then it decreases correspondingly with the broadening of the magnetic flux tube in the exit expander. At the collective beam, relaxation in the plasma a significant fraction of initial beam energy is transferred to suprathermal electrons with energies up to and above the initial beam energy.

Energy distribution of electrons in the plasma stream was carefully studied in our previous experiments on action of hot-electron plasma stream with graphite targets in similar regimes of facility operation [9, 10]. Fig. 2 shows general shape of power density spectrum in the exit mirror (taken from [10]).

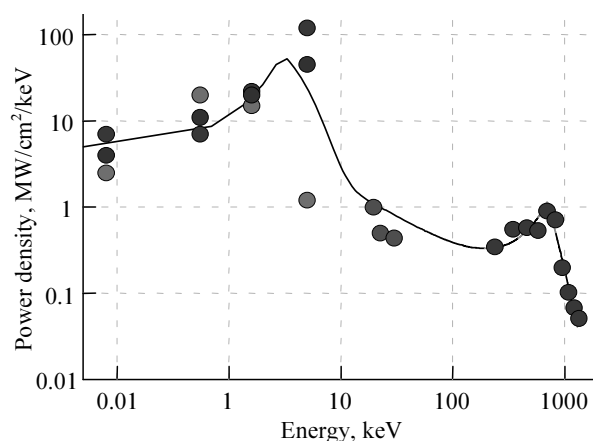


Fig. 2. Energy distribution of power density of irradiating electron stream in the exit mirror [10]

The energy density of the plasma stream was reduced down to ~ 2 MJ/m² in current experiments with lithium-coated targets. This corresponds to estimated transient energy density in ITER ELMs type I regime.

Energy deposition over the target depth was calculated with Monte-Carlo code EMSH [11]. Fig. 3 shows the calculated energy deposition in lithium tar-

get at 2 MJ/m² energy density in the plasma stream and inclined at 30° target.

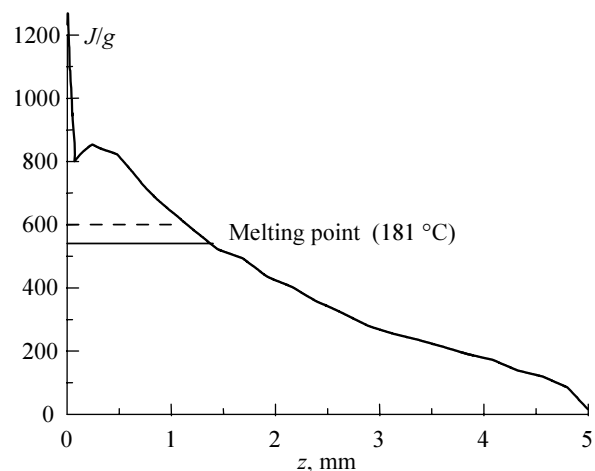


Fig. 3. Calculated energy deposition over depth of lithium under action of plasma hot electrons in GOL-3 facility (power density 2 MJ/m², target inclined at 30°). Horizontal solid and dashed lines correspond to start and end of phase transition, correspondingly. Initially target was at room temperature

At these conditions the lithium surface heats above the melting point and becomes liquid over the depth exceeding 1 mm. therefore the surface of a bulk lithium plasma-facing elements will be unstable and lithium-covered refractory substrate is required instead.

Large density of lithium corona was expected near the target surface. Parameters of this plasma was investigated by several techniques. Visible spectra were recorded with SP-48 spectrograph equipped with CCD camera in intervals of 90 nm width [12]. Absolute sensitivity of this spectral system was calibrated. A single-frame narrowband 2D imaging system consists of interference filter, image converter tube and CCD camera. This system allows spatial distribution measurement of brightness at chosen spectral line. Gating of the image converter tube allows getting exposures from 1 μ s.

3. Experiments with Li-C targets

Several lithium-carbon composite samples was made by different methods:

1. Lithium and sibunit or graphite was heated in argon atmosphere to the temperature 700 °C. In the experiments, these samples were held in special graphite box.

2. Lithium was heated on graphite sample at temperature about 250–300 °C and after melting lithium was smearing for producing homogeneous layer of 0.5–1 mm depth (see Fig. 6).

Special target holder was mounted in exit unit of the GOL-3 facility. Different types of target could be mounted on holder in the view of several diagnostic tools. The total energy density reached the target was measured by blackbody radiation from its surface

(Fig. 4). The method is described in detail in [12]. Following an experiment the energy density was 2.1 MJ/m^2 per shot.

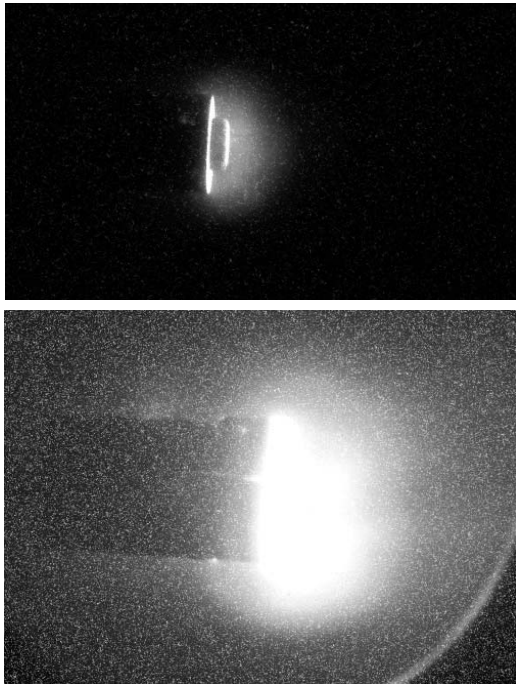


Fig. 4. Plasma radiation of graphite target (top) and sibunit-lithium composite in 4 cm graphite box (bottom) under action of hot plasma stream moving from the right

For first measurements, graphite targets were used, then at the same place lithium-carbon composites were mounted.

First 2 mm depth of lithium-sibunit composites were destroyed after 5 shots. This composite under action of plasma stream is shown in Fig. 4 (bottom).

Second type of targets with lithium films was placed under angle 30° for plasma stream (see Fig. 6).

Spectral system recorded light with wavelength in range 590–680 nm, where bright lithium lines exist. Obtained spectrum is shown in Fig. 5.

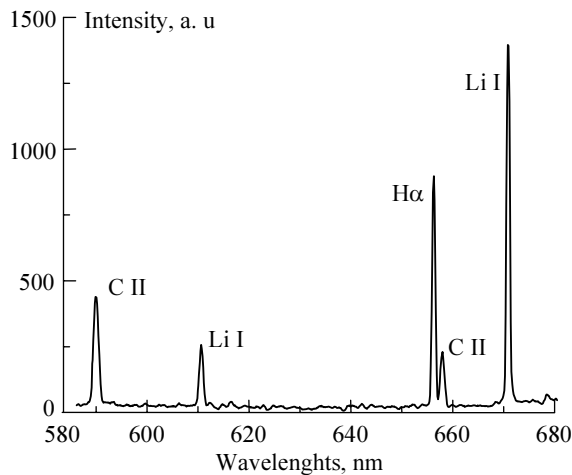


Fig. 5. Spectrum of surface plasma produced near lithium-graphite target under action by power plasma stream

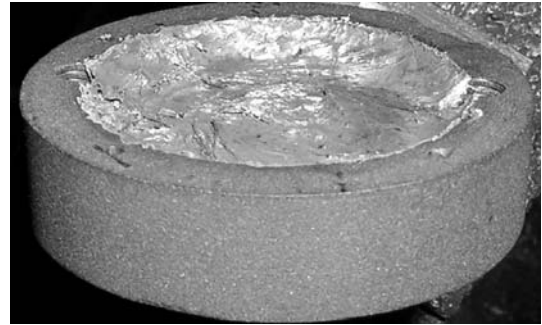


Fig. 6. View of graphite target with lithium films mounted in the exit unit of GOL-3 facility before irradiation from direction of plasma stream

One can determine the plasma electron temperature [13] by relation of intensities of lines Li I 610.36 and 670.78 nm. In different shots temperatures varied within 0.7–1.2 eV. Temperature of lithium plasma is less than temperature of surface plasma near graphite targets (was measured by ratio of C II lines). It corresponds to smaller first ionization potential and higher transmissibility of lithium with respect to carbon.

View of target under action of cold (several eV) foreplasma is shown in Fig. 7.

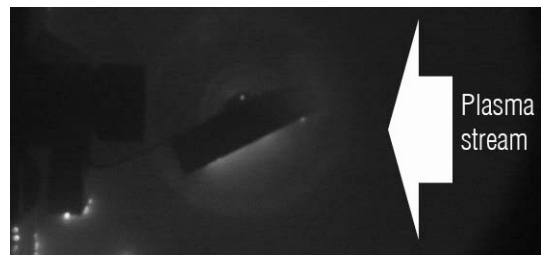


Fig. 7. View of carbon target with lithium films under action of foreplasma in exit unit of GOL-3 facility

First target was irradiated only once and then replaced. Lithium partly evaporates, and remained lithium pills off from graphite, probably because of presence of different temperatures of lithium and graphite under irradiation. Whole lithium from second target evaporated during 6 shots, except of the shadow from graphite board (Fig. 8).

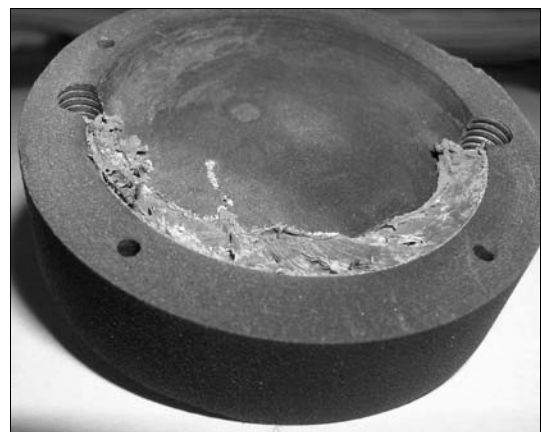


Fig. 8. Graphite target with lithium film after 6 shots

Absolutely calibrated 2D imaging system provided measurements of atomic lithium flux from target. Consider a flux of atoms Φ_A , along a line-of-sight r from surface into a fully ionising plasma. If we assume all the incoming atoms are ionised by electron collisions, between r_1 and r_2 :

$$\Phi_A = \int_{r_1}^{r_2} n_A(r) n_e(r) \langle \sigma_{\text{ionization}} v_e \rangle dr, \quad (1)$$

where $n_A(r)$ and $n_e(r)$ are the density of atoms and electrons. Ionisation rate coefficient $\langle \sigma_{\text{ionization}} v_e \rangle$ is a function of the electron temperature $T_e(r)$. Electron impact excitation of the atom leads to photon emission with the intensity I_A :

$$I_A = \frac{h\nu B}{4\pi} \int_{r_1}^{r_2} n_A(r) n_e(r) \langle \sigma_{\text{excitation}} v_e \rangle dr, \quad (2)$$

where $\langle \sigma_{\text{excitation}} v_e \rangle$ is the electron impact excitation coefficient for the excitation of the upper level of the radiating state, and B is the branching ratio for the radiative decay which leads to the observed photons. Equations (1) and (2) give a relation between the particle fluxes and intensities. Provided the rates do not vary much over the observation volume we may write:

$$\Phi_A = \frac{4\pi}{h\nu B} I_A \frac{\langle \sigma_{\text{ionization}} v_e \rangle}{\langle \sigma_{\text{excitation}} v_e \rangle} = \frac{4\pi}{h\nu} I_A \frac{S}{XB}. \quad (3)$$

Equation (3) enables conversion of the photon flux Φ_A (photons/cm² · s) into the particle flux. The inverse photon efficiency S/XB is the ratio between ionisation rate and the product of excitation rate and branching ratio for the observed electronic transition. For 670.8 nm Li I lines $S/XB = 1/8.6$ was calculated with data from Aladdin database [14].

Estimated atomic lithium flux from the surface was $1 \cdot 10^{20}$ atoms/(cm² · s), it is 3 times smaller with respect to atomic carbon fluxes from graphite targets [15].

4. Conclusion

Several lithium-carbon targets were designed, produced and tested under action of plasma stream. Set of diagnostics was developed and used for investigation parameters of surface plasma near targets. It was shown that lithium erosion depth corresponds

to melting depth. Temperature of surface plasma about 1 eV was measured. Atomic lithium flux from surface was determined. The flux 10^{20} atoms/(cm² · s) cannot explain the erosion value.

Acknowledgements

Authors are grateful to L.V. Zhelnov for help to preparation lithium targets. Authors are grateful to A.V. Arzhannikov, V.T. Astrelin, V.G. Ivanenko, M.V. Ivanstivsky, A.S. Kuznetsov, S.A. Kuznetsov, K.I. Mekler, E.V. Mostipanov, S.S. Popov, A.F. Rovenskikh, S.L. Sinitsky, Yu.S. Sulyaev, V.D. Stepanov, Yu.A. Trunev, and R. Zubairov for help to carry out experiments at the GOL-3 facility.

References

- [1] ITER Physics Basics, Ch. 4, Nuclear Fusion **39**, 2391 (1999).
- [2] G. Federici et al., Nuclear Fusion **41** (12R), 1967 (2001).
- [3] S.V. Mirnov et al., J. of Nuclear Materials **196**, 45 (1992).
- [4] L.G. Golubchikov et al., J. of Nuclear Materials **233-237**, 667 (1996).
- [5] V.A. Evtikhin et al., Plasma Phys. Contr. Fusion **44**, 955 (2002).
- [6] S.V. Mirnov et al., Fusion Engineering and Design **65**, 455 (2003).
- [7] V.F. Surovikin et al., *US patent 4978649*, 1998.
- [8] A. Burdakov et al., Fusion Science and Technology **51** (2T), 106 (2007).
- [9] V.T. Astrelin et al., Nuclear Fusion **37**, 1541 (1997).
- [10] A.V. Arzhannikov et al., Fusion Technology **35** (1T), 146 (1999).
- [11] V. Tayurskiy, *EMSH-code for calculation of electrons and photons of 10 keV – 1 TeV transmitting through the matter*, preprint BINP, 89–16, Novosibirsk, 1989.
- [12] V. T. Astrelin et al., Prib. Tekh. Eksp. **47/2**, 194 (2004).
- [13] H. Griem, *Principles of plasma spectroscopy*, Cambridge, 1997, p. 223.
- [14] <http://www-amdis.iaea.org/ALADDIN>
- [15] S.V. Polosatkin, A.V. Arzhannikov, V.T. Astrelin et al., Prib. Tekh. Eksp. **2**, 100–107 (2008).